stream of nitrogen. The mixture rapidly turned brown-red. It was stirred at −78 °C for 1 h and at room temperature for several hours. The usual workup, including filtration chromatography (10% CH_2Cl_2/pentane) and recrystallization from pentane, gave 0.8 g (1.36 mmol, 47%) of red $(\mu\text{-}CH_3S)(\mu\text{-}C_2H_5HgS)Fe_2(CO)_6$ (mp ~118 °C (dec)): IR (CO region, $CHCl_3$, cm^{-1}) 2070 (s), 2033 (vs), 1995 (sh), 1987 (vs); ^1H NMR ($CDCl_3$) δ 1.31 (t, J_{HH} = 7.5 Hz, $^3J_{HgH}$ = 242.5 Hz, 3 H, CH_3 of Et), 1.645 (q, J_{HH} = 7.5 Hz, $^2J_{HgH}$ = 162.6 Hz, 2 H, CH_2 of Et), 2.15 (s, 3 H, SCH_3); ^{13}C NMR ($CDCl_3$) δ_C 13.033 (CH_3 of Et), 24.189 (SCH_3), 33.43 (CH_2 of Et), and 209.792 (CO). Anal. Calcd for $C_9H_8O_6S_2Fe_2Hg$: C, 18.37; H, 1.37. Found: C, 18.38; H, 1.43.

The addition of 2.9 mmol of CH_3HgCl to such a solution of $(\mu\text{-}LiS)(\mu\text{-}CH_3S)Fe_2(CO)_6$ (from 2.91 mmol of $(\mu\text{-}S_2)Fe_2(CO)_6$ gave, after the usual workup, 0.52 g (0.91 mmol, 31%) of red crystals of $(\mu\text{-}CH_3S)(\mu\text{-}CH_3HgS)Fe_2(CO)_6$ (mp ~137 °C (dec) (recrystallized from 1:1 CH_2Cl_2/pentane)): the mass spctrum showed the molecular ion at m/e 574 (based on ^{200}Hg) and fragment ions corresponding to the successive loss of the six CO ligands; IR (CO region, $CHCl_3$, cm^{-1}) 2073 (s), 2036 (vs), 1998 (sh), 1988 (vs); ^1H NMR ($CDCl_3$) δ 0.85 (s, $^2J_{HgH}$ = 162.5 Hz, CH_3Hg), 2.17 (s, SCH_3); ^{13}C NMR ($CDCl_3$) δ_C 17.507 (CH_3Hg), 24.130 (SCH_3), 209.733 (CO). Anal. Calcd for $C_8H_6O_6S_2Fe_2Hg$: C, 16.72; H, 1.05. Found: C, 16.76; H, 1.11.

The 1:1 reaction of ethyllithium in Et_2O with $(\mu\text{-}S_2)Fe_2(CO)_6$ in THF at −78 °C (2.9-mmol scale), followed by addition of CH_3HgCl to the solution of $(\mu\text{-}LiS)(C_2H_5S)Fe_2(CO)_6$ thus produced, gave 0.75 g (1.274 mmol, 44%) of $(\mu\text{-}C_2H_5S)(\mu\text{-}CH_3HgS)Fe_2(CO)_6$ (mp ~124 °C (dec)), which was identified by melting point and IR and ^1H NMR spectral comparison with the same compound obtained in the reaction of CH_3HgCl with the $LiBEt_3H$-derived $(\mu\text{-}LiS)_2Fe_2(CO)_6$ reagent.

Preparation of $(\mu\text{-}CH_3S)_2Fe_2(CO)_6$ by the $LiAl(O\text{-}t\text{-}Bu)_3H$ Route. A solution of $(\mu\text{-}LiS)_2Fe_2(CO)_6$ in THF at −78 °C was prepared as described above by the reaction of 6 mmol of $LiAl(O\text{-}t\text{-}Bu)_3H$ with 2.91 mmol of $(\mu\text{-}S_2)Fe_2(CO)_6$. To the resulting green solution was added 1 mL (16 mmol) of iodomethane by syringe, which resulted in a rapid color change from green to light red. The reaction mixture was stirred briefly at −78 °C and for 90 :min at room temperature. It then was evaporated at reduced pressure. The residue was dissolved in pentane and submitted to filtration chromatography. Elution with pentane gave a red solid which was recrystallized from pentane: 0.53 g (1.55 mmol, 53%); mp 67–68 °C; ^1H NMR (60 MHz, $CHCl_3$) δ 1.62 (s), 2.12 (s). This is indicative of isomer XIIa of $(\mu\text{-}CH_3S)_2Fe_2(CO)_6$ (lit.[7] mp 65–67.5 °C).

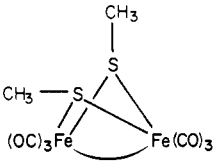

XIIa

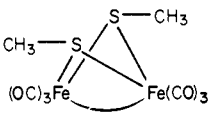

XIIb

Elution with 10% CH_2Cl_2/pentane gave a red solid which was recrystallized from pentane: 0.32 g (0.86 mmol, 29%); mp 105–106 °C. The 60-MHz proton NMR spectrum (in $CHCl_3$) of this product showed a singlet at δ 2.05, indicative of isomer XIIb of $(\mu\text{-}CH_3S)_2Fe_2(CO)_6$ (lit.[7] mp 101.5–103.5 °C). The total product yield thus was 82%.

Reaction of Potassium Hydride-Derived $(\mu\text{-}KS)_2Fe_2(CO)_6$ with Triethylborane and Methylmercuric Chloride. The reaction of KH (7.93 mmol) with 2.91 mmol of $(\mu\text{-}S_2)Fe_2(CO)_6$ in 50 mL of THF, using the procedure described above, served to give $(\mu\text{-}KS)_2Fe_2(CO)_6$. The mixture was filtered to give a brown-green solution. To this solution was added a solution of Et_3B in THF (prepared by the reaction of ethylene with 10.7 mL of 0.56 M BH_3 (6 mmol) in THF). No color change was noted. Then 0.73 g (2.91 mmol) of CH_3HgCl was added as the solid, all at once. The reaction mixture soon turned brown-red. After it had been stirred at room temperature for 2 h, the usual workup followed. Filtration chromatography gave trace amounts of $(\mu\text{-}S_2)Fe_2(CO)_6$ and $S_2Fe_3(CO)_9$ (elution with pentane). Elution with 10% CH_2Cl_2/pentane gave an orange and a red band. The products in these bands were isolated and recrystallized from pentane and 10% CH_2Cl_2, respectively. They were identified (mp, mmp, IR, NMR) as $(\mu\text{-}C_2H_5S)(\mu\text{-}CH_3HgS)Fe_2(CO)_6$ (0.15 g, 0.25 mmol, 9% yield, based on $(\mu\text{-}S_2)Fe_2(CO)_6$) and $(\mu\text{-}CH_3HgS)_2Fe_2(CO)_6$ (0.52 g, 0.67 mmol, 23% yield).

Acknowledgment. We are grateful to the National Science Foundation for generous support of this research. Special thanks are due to Professor D. S. Matteson for his useful suggestions concerning mechanism. L.-C.S. is a visiting scholar on leave from the Department of Chemistry, Nankai University, Tian-Jin, People's Republic of China.

Synthesis and Characterization of a Novel Family of Dimeric Nickel(II) Complexes—Bimetallic Species Separated by a Persistent Void

Daryle H. Busch,* Gary G. Christoph,* L. Lawrence Zimmer, Susan C. Jackels, Joseph J. Grzybowski, Robert C. Callahan, Massaki Kojima, Katherine Anne Holter, Jan Mocak, Norman Herron, Madhav Chavan, and Wayne P. Schammel

Contribution from Evans Chemical Laboratory, The Ohio State University, Columbus, Ohio 43210. *Received November 20, 1980*

Abstract: A novel family of ligands has been synthesized and characterized as their nickel(II) complexes. The ligands are comprised of pairs of 16-membered macrocyclic ligating sites held in an approximate face-to-face orientation by various bridging moieties, including $(CH_2)_n$, where n = 2–8, *m*- and *p*-xylyl, and duryl. They are prepared by condensation reactions from monomeric macrocyclic precursor complexes. The same reactions also yield monomeric *lacunar* complexes in many cases. The dimeric bimetallic complexes were purified by fractional crystallization and/or chromatography and characterized by the usual physical means. A specific route has been devised for dimer synthesis. On an NMR time scale the structures typically possess two symmetry elements, e.g., a mirror plane and an inversion center. An X-ray structure determination of the *m*-xylene-bridged complex reveals the details of the structure: the Ni–N distance and the related bond angles are normal for square-planar diamagnetic nickel(II) (Ni–N = 1.87 (average) Å, N–Ni–N angle (average) = 89.9°). Of greatest importance, the structure shows the size and nature of the persistent void caused by the rigid components of the molecule. The metal ions are 13.6 Å apart, separated by an empty cavity that is from 3.87 to 6.18 Å wide.

The cooperative functioning of pairs or quartets of metal atoms in a substantial array of natural products (e.g., hemoglobin, cytochrome oxidase, hemerythrin, hemocyanine, and laccase) has attracted attention to dimeric complexes in which the metal ion proximity is enforced by the ligands. Side-by-side dimers based on the systems first prepared by Pilkington and Robson[1] have

0002-7863/81/1503-5107$01.25/0

Scheme I.

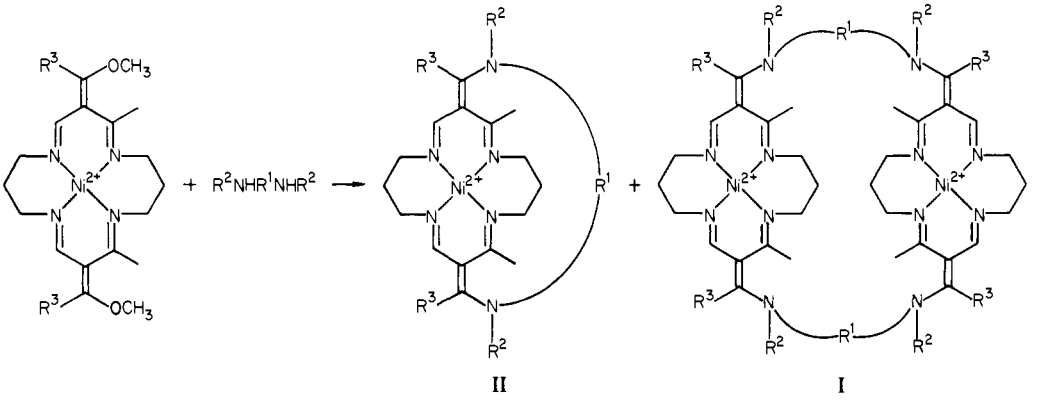

II I

received much attention.[2-5] Face-to-face dimers are represented by dimeric porphyrins[6] that are of much current interest in electrochemical applications.[7] A major source of interest in bimetallic dimers resides in the possibility of producing complementary 2-electron processes and of improving the kinetic behavior of polyelectron processes, notably O_2 reduction. Of paramount importance to basic chemistry is the use of bimetallic dimers as vehicles for the continuing study of the fundamental aspects of electron transfer between metal ion centers.[8] The dimers reported here are best described as face-to-face bimetallic species. Distinct series of dimer-producing ligands are rare, and the new series reported here has many readily varied structural parameters. The easily controlled cavity size and the novel face-to-face arrangement suggest that these complexes will find many applications in the areas mentioned above. The new complexes are doubly interesting because of the presence of a persistent void[9] within the ligand structure and between the metal ions. Other studies in our laboratories[10] suggest that various molecular species may enter the void, thereby greatly increasing the possible research applications that might be made of the complexes. The template syntheses of a number of ligands, in the form of their nickel(II) complexes, are reported here. The structures have been established by a variety of definitive and inferential means, including an X-ray crystal structure determination.

Results and Discussion

Synthesis. The usual synthetic route to the new dimers (structure I) is given in Scheme I. The principal structural variation reported here involves changes in the bridging group R^1. As reported earlier,[11] a number of the dimers are produced along with monomeric *lacunar* ligands (structure II).[12-14] The details

Scheme II

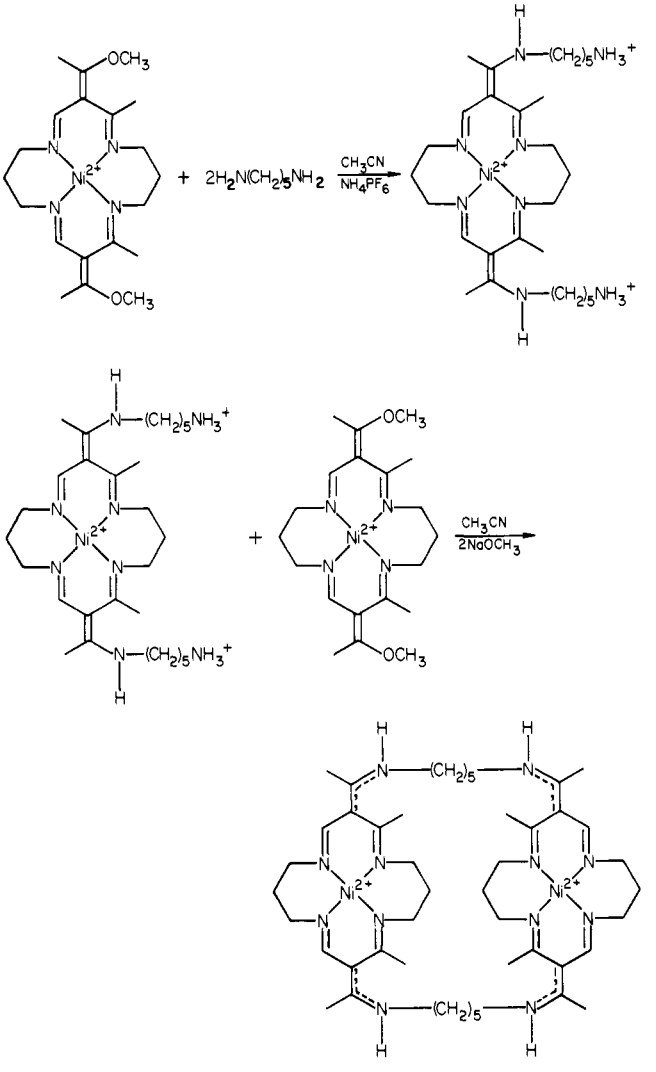

of the synthetic reactions and the separation and identification of the monomer–dimer isomers are presented in a separate paper.[11] These include cases where $R^3 = CH_3$ and the bridging group is $NH(CH_2)_nNH$ (n = 4–8), $(NH)_2p$-xylyl, $(NH)_2m$-xylyl, $CH_3N(CH_2)_2NCH_3$, and $(NH)_2C_7Fl$ (the bridging group derived from 9,9-bis(3-aminopropyl)fluorene). The characterization of these compounds is presented here. In addition to the dimers separated

(1) Pilkington, N. H.; Robson, R. *Aust. J. Chem.* **1970**, *23*, 2225–2236.
(2) Fenton, D. E.; Gayda, S. E. *J. Chem. Soc., Dalton Trans.* **1977**, 2109–2115.
(3) Glick, M. D.; Lintvedt, R. L.; Anderson, T. J.; Mack, J. L. *Inorg. Chem.* **1976**, *15*, 2258–2262.
(4) Gagne, R. R.; Sprio, C. L. *J. Am. Chem.* **1980**, *102*, 1443–1444.
(5) Okawa, H.; Tanaka, M.; Kida, S. *Chem. Lett.* **1974**, 987–988.
(6) Ogoshi, H.; Sugimoto, H.; Yoshida, A. Hukusokan Kagaku Toronkai Koen Yoshishu, 8th **1975**, 239–243. Collman, J. P.; Elliott, C. M.; Halbert, T. R.; Tovrog, B. S. *Proc. Natl. Acad. Sci. U.S.A.* **1977**, *74*, 18–22. Chang, C. K. "Biochemical and Clinical Aspects of Oxygen", Caughey, W. S., Ed.; Academic Press: New York, 1979; pp 437–455.
(7) Collman, J. P.; Marrocco, Denisevick, P.; Koval, C.; Anson, F. C. *J. Electroanal. Chem.* **1979**, *101*, 117–122.
(8) Taube, H. *Adv. Chem. Ser.* **1977**, *No. 162*, 127–144.
(9) Busch, D. H.; Olszanski, D. J.; Stevens, J. C.; Schammel, W. P.; Kojima, M.; Herron, N.; Zimmer, L. L.; Holter, K. A.; Mocak, J. *J. Am. Chem. Soc.*, in press.
(10) Zimmer, L. L., thesis, The Ohio State University, Columbus, Ohio, 1979.
(11) Busch, D. H.; Jackels, S. C.; Callahan, R. C.; Grzybowski, J. J.; Zimmer, L. L.; Kojima, M.; Olszanski, D. J.; Mertes, K. B.; Christoph, G. G.; Schammel, W. P.; Stevens, J. C.; Holter, K. A.; Mocak, J., submitted for publication.
(12) Schammel, W. P.; Mertes, K. B.; Christoph, G. G.; Busch, D. H. *J. Am. Chem. Soc.* **1979**, *101*, 1622–1673.
(13) Stevens, J. C.; Jackson, P. J.; Schammel, W. P.; Christoph, G. G.; Busch, D. H. *J. Am. Chem. Soc.* **1980**, *102*, 3283–3285.
(14) Stevens, J. C.; Busch, D. H. *J. Am. Chem. Soc.* **1980**, *102*, 3285–3287.

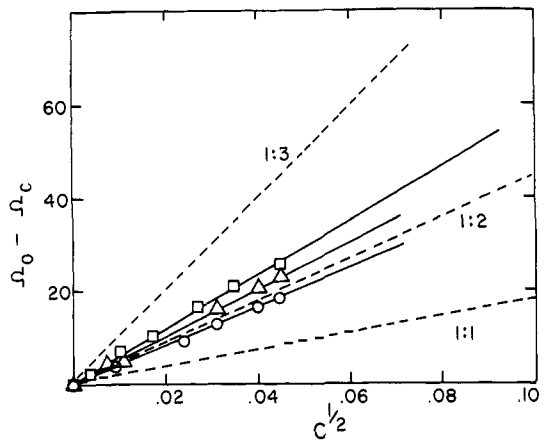

Figure 1. Onsager plots for monomeric *lacunar* and dimeric bimetallic nickel(II) complexes in acetonitrile: (a) monomeric $[Ni\{(CH_2)_4(NHE-thi)_2Me_2[16]tetraeneN_4\}](PF_6)_2$, ○; (b) dimeric $[Ni_2\{(CH_2)_4(NHE-thi)_2Me_2[16]tetreneN_4\}_2](PF_6)_4$, □; (c) dimeric $[Ni_2\{(CH_2)_3(NHE-thi)_2Me_2[16]tetraeneN_4\}_2](PF_6)_4$, △.

from isomeric mixtures, other dimers are the exclusive products of reactions utilizing certain linking groups. These include the relatively short chains, ethylene and trimethylene, which appear to be too short to span the bridging positions for a monomeric *lacunar* structure and relatively bulky aromatic groups. The steric demands of the duryl group are sufficiently great to produce only dimers. These exclusive dimeric products are also discussed in detail here.

Establishing the Dimeric Structure. The ultimate proof that these compounds are indeed dimers was provided by an X-ray crystal structure determination, whose results are presented below. Other examples have been established as members of the series by a variety of means.

A selective synthetic scheme has been devised and used for the cases of the pentamethylene and C_7Fl bridging groups (Scheme II). This was accomplished by first using an excess of diamine (1,5-diaminopentane, in the example) to produce the unbridged bis complex. Reaction of this complex with a second mole of the methyl vinyl ether derivative gave the desired dimeric complex.

As was discussed in the report on the related *lacunar* complexes,[11] a number of correlative techniques apply to the problem of distinguishing between monomers and dimers. The use of molecular weight techniques and conductance methods have failed, probably because of the high charge of the dimeric cation. Of course, the values of the molar conductance observed for the dimers are consistent with either diunivalent electrolytes or tetraunivalent electrolytes;[15] however, one usually hopes to make a distinction between oligomerization isomers on the basis of Onsager plots.[16] The Onsager plot for the *m*-xylyl-bridged dimer in acetonitrile, whose structure is known from the X-ray study, shows a slope of 602 ± 28 Ω^{-1} $mol^{-1.5}$ $cm^{3.5}$. This is about 100 units larger than the value for the corresponding monomer but not nearly as large as expected for a 4:1 electrolyte. Parallel results were obtained with the tetramethylene and C_7Fl-bridged species in acetonitrile. The relationship of the data to typical electrolyte types is shown in Figure 1. It would be very interesting to know the source of the closely similar conductivity parameters for the monomers and dimers. The obvious suspicion arises that ion pairing may be greatly enhanced by the cavity.

Direct molecular weight determinations are possible on the species that can be converted to neutral molecules. For these dimeric bimetallic complexes, four protons must be removed from the ligand to produce the neutral species (eq 1). A simple procedure involving addition of 4 equiv of $NaOCH_3$ in acetonitrile produces a deep red solution of the neutral complex.[9] Evaporation and benzene extraction gives a clear red solution which on evaporation produces the desired neutral materials. With some

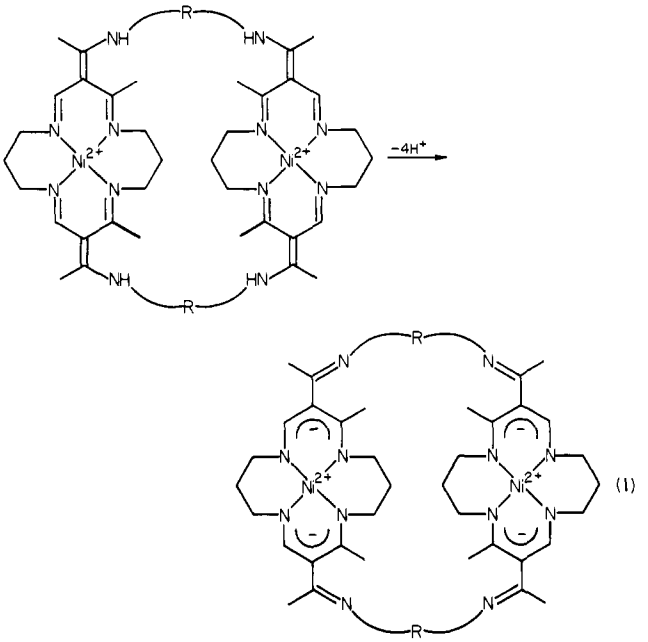

difficulty, this has been accomplished for the cases of the $(NH)_2(CH_2)_7$, $(NH)_2(CH_2)_8$, $(NH)_2$duryl, $(NH)_2$*m*-xylyl, and $(NH)_2C_7Fl$ linked dimers. Molecular weights were estimated by vapor pressure osmometry; mass spectroscopy using conventional direct probe methods has generally failed, apparently because decomposition precedes vaporization. The results were as follows: calcd for neutral derivative of $(NH)_2(CH_2)_7$-linked dimer 966.7 daltons, found 960 daltons; calcd for neutral derivative of $(NH)_2(CH_2)_8$-linked dimer 994.7 daltons, found 985 daltons; calcd for neutral derivative of $(NH)_2$*m*-xylyl-linked dimer 978.62 daltons, found 962 daltons; calcd for neutral derivative of $(NH)_2$duryl-linked dimer 1090.8 daltons, found 1125 daltons; calcd for $(NH)_2C_7Fl$ dimer 1267 daltons, found 1241 daltons.

The simplest convincing demonstration that a given structure is dimeric comes from an ion exchange experiment.[11] If a mixture of monomeric *lacunar* complex and dimeric bimetallic complexes is adsorbed on a CM-Sephadex column from aqueous solution, the monomer is easily eluted with 0.2 M aqueous Na_2SO_4 while the dimer is not. The dimer can be eluted with 0.4 M aqueous Na_2SO_4.

Characterization. Satisfactory elemental analyses were obtained for all of the complexes (see Experimental Section and ref 11). Infrared spectra of the dimeric complexes have the same general features as those of the related monomers[9,11] with the only major differences appearing in the fingerprint region. In general, the dimeric complexes show fewer sharp absorptions than the monomers.

Proton NMR data for the complexes are listed in Table I and are similar to those of the corresponding monomeric species.[9] The ^1H NMR spectra of the $(NH)_2$*m*-xylyl- and $(NMe)_2$duryl-bridged dimeric complexes are representative and appear in Figure 2.

With a single exception, the ^{13}C NMR spectra of all the dimers show the same number of resonances as were observed for the corresponding monomers.[9] This indicates the presence of two symmetry elements within the molecule. As will be described in the discussion of the structural analysis of the anomalous dimeric $(NH)_2$*m*-xylyl-bridged species, these elements are probably an inversion center relating to two metal coordinating macrocycles and a mirror plane through the macrocycles and the metal centers. The resonances are listed in Table I, and the spectrum of the dimeric $(NMe)_2$duryl-bridged complex appears in Figure 3. Assignments can be made as presented for the monomers.[9] As mentioned above, the spectrum of the dimeric $(NH)_2$*m*-xylyl complex is not as simple as the others. This may be due to the presence in solution of several isomeric species which are not interconverting on the NMR time scale. The X-ray crystal structure for the PF_6^- salt of the $(NH)_2$*m*-xylyl-bridged complex

(15) Geary, W. J. *Coord. Chem. Rev.* **1971**, *7*, 81–172.
(16) Feltham, R. D.; Hayter, R. G. *J. Chem. Soc. A* **1964**, 4587–4591.

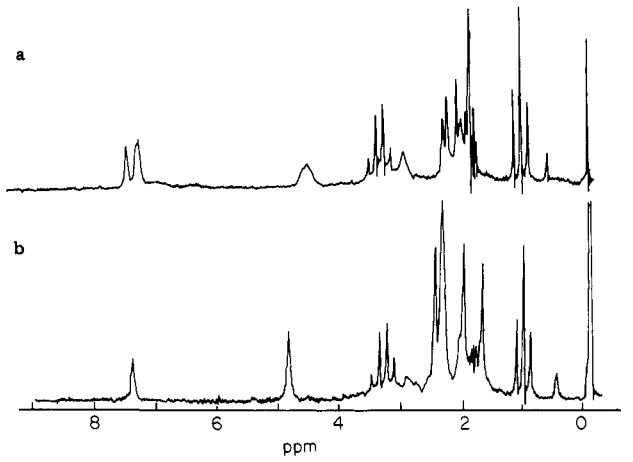

Figure 2. Proton NMR spectra of (a) $[Ni_2\{(m\text{-xylyl})(NHEthi)_2Me_2[16]tetraeneN_4\}_2](PF_6)_4$ and (b) $[Ni_2\{(duryl)(NHEthi)_2Me_2[16]tetraeneN_4\}_2](PF_6)_4$.

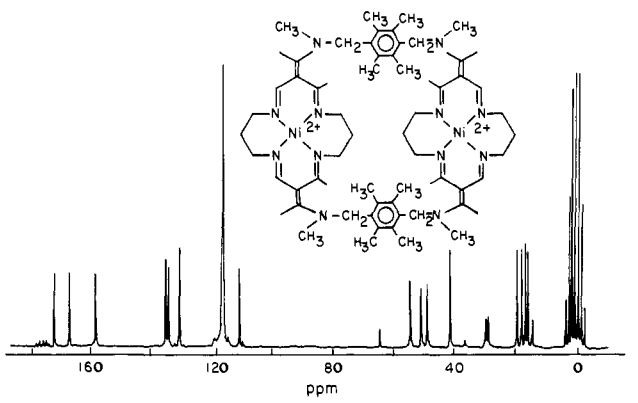

Figure 3. Carbon-13 NMR spectrum of the dimeric bimetallic complex containing (NCH_3)duryl linkages.

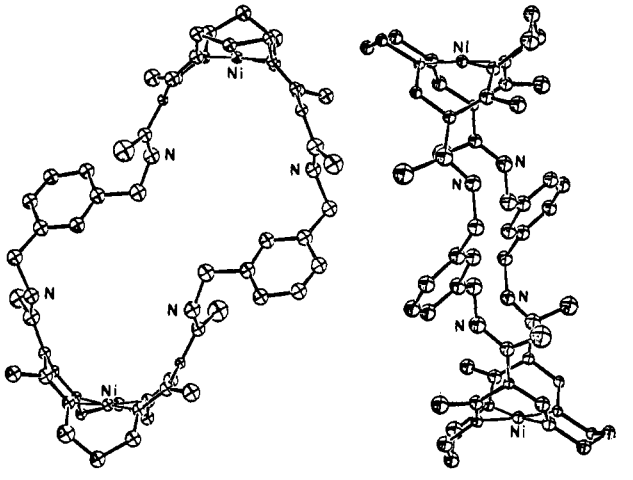

Figure 4. ORTEP drawings of the structure of the dimeric dimetallic complex $[Ni_2\{(m\text{-xylyl})(NHEthi)_2Me_2[16]tetraeneN_4\}_2](PF_6)_4 \cdot 2(CH_3COCH_3)$.

shows that the mirror plane, which might be expected for this molecule, is obviated in the solid state by a skewing of the macrocycle planes. This is evident in the ORTEP view directly into the cavity of the complex (Figure 4a). One might have expected the cross section of the cavity, as viewed from this position, to be approximately rectangular, with the planes of the macrocycles defining the short sides. However, this cross section is better described as a parallelogram. This source of lowered symmetry is not expected to persist in solution, leading one to suspect an alternative source of isomerism. Since the phenomenon occurs with the unsymmetrical *m*-xylene but has not been observed with

Table I. Proton NMR and Carbon-13 NMR Data for the Dimeric Bimetallic Nickel(II) Complexes[a]

compd		proton NMR data[b]				^{13}C NMR data
bridge link	N substituent	methyl	methylene	vinyl or aromatic	NH	
$(CH_2)_2$	H	2.30, 2.03	2.07,[c] 2.73,[c] 3.2,[c] 3.58[b]	7.53		169.3, 161.1, 113.5, 65.0, 63.9, 62.8, 61.7, 57.3, 52.0, 46.2, 30.8, 30.7, 20.9, 15.4[e]
$(CH_2)_3$	H	2.40, 2.23	2.10, 2.83,[c] 3.1,[c] 3.30,[c] 3.53,[c] 3.66[c]	7.59	6.56	169.3, 168.8, 160.2, 113.6, 56.9, 51.8, 42.6, 31.2, 30.4,[f] 30.4,[f] 20.7, 14.8[b]
$(CH_2)_4$	H	2.42, 2.26	2.0,[c,d] 3.3[d]	7.62	6.3	169.9, 168.7, 160.5, 113.0, 57.2, 52.1, 46.4, 31.0, 30.7, 27.2, 20.9, 15.7[b]
$(CH_2)_5$	H	2.41, 2.22	1.7,[c,d] 3.5[d]	7.57	6.7	169.2, 168.7, 160.1, 113.0, 57.0, 51.9, 45.6, 31.1, 30.6, 29.9, 24.8, 20.7, 15.1[b]
$(CH_2)_7$	H	2.46, 2.26	1.54,[c] 1.86,[c] 2.86,[c] 3.21,[c] 3.5[d]	7.64	6.8	168.1, 159.8, 118.2, 112.4, 56.1, 51.2, 45.7, 30.5, 30.0, 29.6, 27.1, 20.5, 15.1[b]
$(CH_2)_8$	H	2.40, 2.20	1.43, 1.83,[d] 3.1,[c] 3.5[d]	7.59	6.7	168.2, 160.1, 118.2, 112.3, 56.3, 51.4, 46.1, 30.6, 30.2, 29.6, 27.4, 20.9, 15.5[b]
C_7H_2	H	1.72, 2.32	1.1,[c] 1.9,[c] 2.2,[c] 3.3[c]	7.5,[c] 7.67, 7.8,[c] 7.9[c]	6.7	
m-xylene	H	2.08, 2.25, 2.41, 2.52	3.0,[d] 4.6[d]	7.42, 7.55		170.1, 169.3, 169.2, 168.9, 168.7, 168.2, 160.7, 139.5, 138.5, 137.9, 131.4, 131.1, 130.8, 130.3, 129.2, 128.2, 128.0, 127.7, 113.2, 56.9, 51.9, 50.0, 49.0, 31.0, 30.4, 20.8, 15.4[e]
p-xylene	H	2.03, 2.37	2.80, 3.05,[c] 4.60	7.43, 7.55		168.6, 168.2, 160.7, 136.9, 131.5, 130.3, 112.9, 56.8, 51.7, 50.3, 30.9, 30.4, 20.7, 15.4[e]
p-duryl	H	1.73, 2.23, 2.37, 2.50	3.05,[c] 4.88	7.58		168.1, 167.9, 160.6, 136.4, 135.0, 133.0, 112.3, 66.3, 56.5,[b] 51.5, 30.3, 29.9, 19.9, 17.1, 16.8, 15.7
p-duryl	CH_3	1.8, 2.10, 2.47, 2.57	3.0,[c] 4.95	7.53		169.4, 168.5, 159.8, 136.6, 136.0, 132.3, 112.6, 66.3, 56.3, 52.7, 50.6, 43.2, 31.0, 30.3, 20.8, 19.3, 18.0, 17.2, 15.6[b]

[a] As PF_6^- salts. [b] Data taken in CD_3CN solution, relative to Me_4Si. [c] Broad. [d] Multiplet. [e] Data taken in CD_3NO_2 solution. [f] Peaks not resolved.

Table II. Electrochemical Data for the Dimeric Bimetallic Nickel(II) Complexes[j]

ligand structure		oxidation				reduction			
bridge links	*N* substituent	$E_{1/2}$, V	Δ_1,[a] mV	E_p, V	Δ_2,[a] mV	$E_{1/2}$, V	Δ_1,[a] mV	E_p, V	Δ_2,[a] mV
$(CH_2)_2$	H			~0.81[i]					
$(CH_2)_3$	H	0.88	75	0.91	83	−1.86[h]	89	−1.97[g]	221
		1.16	102	1.23[g]	97			−2.79[d,f]	
		1.74	150	1.76[b]	117				
$(CH_2)_4$	H	0.87	63	0.90	65	−1.82	113	−1.925[g]	191
		1.15	110	1.20[g]	112	−2.69[d]		−2.80[g]	
$(CH_2)_5$	H	0.85	65	0.89	70	−1.89	80	−1.93[g]	100
		d		1.19[g]	90	*d*, *e*		−2.9	115
$(CH_2)_7$	H	*c*		0.85	70	−1.89	60	−1.94	
		c		1.17	100	−2.43[d]			
								−2.72	170
$(CH_2)_8$	H	0.82	50	0.83	60	−1.90	80	−1.94[b]	
		1.16	60	1.18	110			−2.72	170
				1.60					
C_7Fl	H	0.91	90	0.96[e]	110	−1.89	95	−1.94	85
		f		1.22	75	*f*		−2.65[g]	90
		f		1.39[f]	50				
m-xylyl	H	0.88	85	0.925	100	−1.83	85	1.89[g]	110
		f		1.23[g]		*h*			
p-xylyl	H	0.88	80	0.93	88	−1.84	90	−1.87[g]	90
		f		1.23[g]		*f*		−2.72	90
p-duryl	H	0.890	70	0.960	73	*f*		−1.85[d]	
		1.190	100	1.35[g]	180	*f*		−2.8[d]	
		f		1.75	185				
p-duryl	CH_3	0.780	80	0.830	77	−1.88	100	−1.93	90
		1.06	55	1.130	60	*f*		−2.22[g]	75
		f		1.75[g]	90	*f*		−2.82	120

[a] RPE scan rate, 5 mV s^{-1}; CV scan rate, 50 mV s^{-1}; $\Delta_1 = |E_{3/4} - E_{1/4}|$, (60 mV for reversible process) from RPE; $\Delta_2 = |E_p - E_{p/2}|$ from CV. [b] Broad. [c] Asymmetric wave. [d] Indistinct wave, approximate value only. [e] Adsorption occurred. [f] Further scanning resulted in electrode inhibition. [g] No counter peak in CV. [h] Further reduction is scan rate dependent. [i] System very poorly behaved; only this process could be detected. [j] CH_3CN solution; 0.1 N $(n\text{-}Bu)_4NBF_4$ supporting electrolyte; $Ag/AgNO_3$ (0.1 N) reference electrode.

the symmetrical *p*-xylyl-linked species, isomerism may result from different orientations of the linking groups. This rationale seems improbable, however, because the rate of interchange between such conformational isomers should be rapid on the NMR time scale. It may be that the *m*-xylyl bridges are not free to rotate individually about their respective linkages but are coupled in a manner similar to a pair of ellipsoidal gears, which precludes a mirrored disposition.

This dimeric ligand structure permits a mode of geometrical isomerism that would not be subject to isomerization under mild conditions. Because the linking groups rise from atoms that are off center with regard to the parent macrocycles, the links may orient the two macrocycles either in an offset array or more nearly over each other. This can be illustrated by referring to the side-on ORTEP view given in Figure 4. This is the *offset* structure and is represented more simply in structure III. The other isomer,

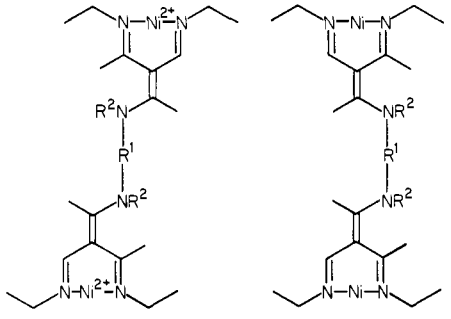

III IV

in which NiN_4 planes are more or less over each other, is shown in side view in structure IV. To date, no compelling evidence has been found for such noninterconvertible isomers.

An outstanding feature of the ^{13}C NMR spectra of these dimeric complexes is the fact that the macrocycle methyl resonances are separated by approximately 5 ppm. On the basis of previous arguments,[11] this observation is interpreted to mean that the dimers are all of the "*lid-on*" type with respect to the orientation of groups around the bridge nitrogen atoms (structures V and VI). The alternative "*lid-off*" orientation is unlikely for the dimers because of the bulky groups joined by the bridge.

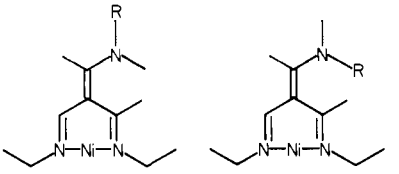

lid-on isomer V lid-off isomer VI

Electrochemical studies have shown that the redox behavior of the dimeric complexes is very similar to that of the monomers with little dependence on the nature of the linking group (Table IIA). The first oxidation potential listed for each dimeric complex in Table II, (E = 0.9 V) is assigned (by analogy with the related monomeric *lacunar* complexes[9]) to the metal-based $Ni^{II/III}$ couple. The assignment is supported by the relatively good reversibility of this couple and is based on bulk electrochemical oxidation at this potential and identification of the product as a nickel(III) species by EPR. When the nickel(II) is replaced by M(II) (either iron(II) or cobalt(II)), the potential assigned to the $Ni^{II/III}$ couple clearly disappears to be replaced by $M^{II/III}$ while the rest of the electrochemistry remains essentially unchanged, indicating its basis in ligand phenomena. Changing the bridge nitrogen substituent from hydrogen to methyl in the case of the duryl-bridging group causes a shift of 110 mV more negative; this behavior accords with that observed among the monomeric examples.[11] It is interesting to note that the dimeric $(NH)_2$*p*-xylyl species has a half-wave potential of +0.880 V, which falls in the normal range for this type of macrocyclic nickel(II) complex. This is in marked contrast to the exceptional behavior of the corresponding monomer which has the anomalously high potential of >1.04.

As noted above the presence of two metal ions in the dimers produces no significant broadening of the $Ni^{II/III}$ wave over that observed for monomers and certainly no splitting of the wave into two components is observed. Coulometric n values for this wave indicate a two electron per dimer process, clearly indicating that

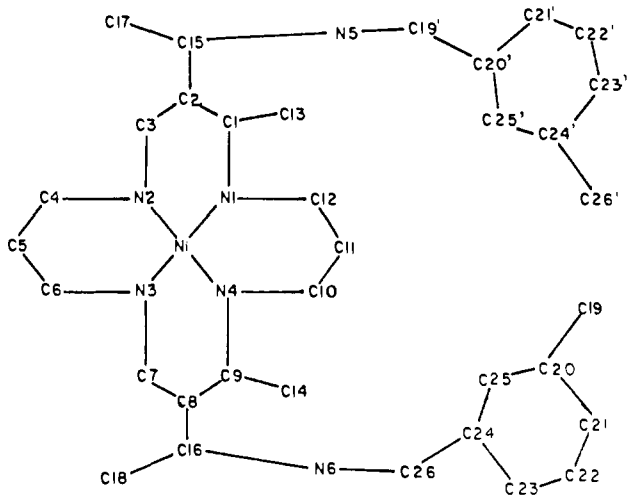

Figure 5. Numbering scheme for dimeric nickel(II) complex.

Table III. Bond Distances (Å) For Dimeric Nickel(II) Complex[a]

Ni-N1	1.877	C5-C6	1.57	C23-C24	1.44
Ni-N2	1.902	C7-C8	1.43	C24-C25	1.38
Ni-N3	1.868	C8-C9	1.47	C24-C26	1.52
Ni-N4	1.851	C8-C16	1.42	C26-N6	1.52
N1-C1	1.33	C9-C14	1.55	P1-F1	1.578
N1-C12	1.46	C10-C11	1.48	P1-F2	1.598
N2-C3	1.26	C11-C12	1.51	P1-F3	1.564
N2-C4	1.47	C15-C17	1.52	P1-F4	1.594
N3-C6	1.49	C15-N5	1.34	P1-F5	1.590
N3-C7	1.30	C16-C18	1.52	P1-F6	1.558
N4-C9	1.29	C16-N6	1.35	P2-F7	1.574
N4-C10	1.53	C19-N5	1.44	P2-F8	1.544
C1-C2	1.47	C19-C20	1.54	P2-F9	1.541
C1-C13	1.51	C20-C21	1.45	P2-F10	1.567
C2-C3	1.44	C20-C25	1.37	P2-F11	1.491
C2-C15	1.38	C21-C22	1.42	P2-F12	1.524
C4-C5	1.52	C22-C23	1.34		

[a] The average estimated standard deviations in the Ni-N distances are ±0.01 Å, while the esd's in the internuclear distances in the remainder of the cation range from ±0.02 to ±0.03 Å. The disorder in the PF_6^- anions renders their distances uncertain to ±0.06 Å.

the two metal ions are electrochemically independent. This lack of metal–metal interaction is to be expected in light of the large nonconjugated separation of the ions (M–M = 13.6 Å for the *m*-xylyl derivative).

X-ray Structure. The complex $[Ni_2\{(m\text{-xylyl(NHEthi)}_2]$Me-[16]tetraeneN$_4\}_2](PF_6)_4 \cdot 4CH_3COCH_3$ was subjected to a complete single-crystal X-ray diffraction structural analysis. Specific details of the solution and refinement procedures are found in the Experimental Section of this work. ORTEP drawings of the molecule appear in Figure 4. The numbering scheme for the molecule is shown in Figure 5, and the relevant bond distances and angles are listed in Tables III and IV.

Despite numerous difficulties encountered in the structural analysis and the resultant high discrepancy indices (vide infra), a number of significant observations can be made regarding the complex. The most striking feature is the dimeric nature of the molecule. Two macrocyclic species are linked by *m*-xylene bridges with the two halves of the molecule related by a crystallographic inversion center. The xylyl groups are, by symmetry, parallel as are the macrocyclic N_4 planes. The nickel(II) ions are 0.07 Å out of the N_4 planes (away from the molecular center) with an average nickel–nitrogen distance of 1.87 Å. These values compare favorably with those of the monomeric $(NH)_2p$-xylyl-bridged nickel complex, 0.04 and 1.87 Å, respectively.[12] The six-membered rings containing the macrocyclic side chain below the xylene groups are in boat conformations whereas the other six-membered rings are in the chair form. This is consistent with expected steric interactions between the bridging group and the macrocycle. The

Table IV. Bond Angles[a] (Deg) for Dimeric Nickel(II) Complex

N2-Ni-N1	89.2	C16-C8-C7	118.6
N4-Ni-N1	89.9	C16-C8-C9	124.0
N3-Ni-N2	91.3	C8-C9-N4	120.6
N4-Ni-N3	89.3	C14-C9-N4	118.8
C1-N1-Ni	120.3	C14-C9-C8	120.0
C12-N1-Ni	119.4	C11-C10-N4	108.7
C12-N1-C1	120.3	C12-C11-C10	111.4
C3-N2-Ni	117.1	C11-C12-N1	111.5
C4-N2-Ni	122.2	C17-C15-N5	118.7
C4-N2-C3	120.3	C17-C15-C2	120.7
C6-N3-Ni	122.1	N5-C15-C2	120.4
C7-N3-Ni	119.6	C18-C16-N6	119.7
C7-N3-C6	117.2	C18-C16-C8	121.9
C9-N4-Ni	120.2	N6-C16-C8	118.4
C10-N4-Ni	120.6	C19-N5-C15	126.2
C10-N4-C9	119.1	C26-N6-C16	125.8
C2-C1-N1	121.7	C20-C19-N5	114.8
C13-C1-N1	119.9	C21-C20-C19	118.2
C13-C1-C2	117.1	C21-C20-C25	121.3
C3-C2-C1	112.9	C25-C20-C19	120.4
C15-C2-C1	122.7	C22-C21-C20	117.0
C15-C2-C3	124.4	C23-C22-C21	119.9
C2-C3-N2	127.9	C24-C23-C22	123.2
C5-C4-N2	111.9	C25-C24-C23	117.5
C6-C5-C4	111.3	C26-C24-C23	120.2
C5-C6-N3	111.0	C26-C24-C25	121.9
C8-C7-N3	120.8	C24-C25-C20	121.1
C9-C8-C7	117.1	C24-C26-N6	109.3

[a] The uncertainties in the bond angles involving the Ni(II) center are ±0.3°; those for other combinations of atoms average ±0.7°.

dihedral angle between the N_4 macrocycle plane and the plane of the xylyl ring is 54°.

The nickel(II) ions are 13.6 Å apart from center to center, of which 12.8 Å is the vertical and 4.6 Å is the horizontal (parallel to the N_4 plane) displacement. The point of nearest approach across the cavity is between C19 and C26, the benzylic carbons, at a distance of 3.87 Å. The distances between nonbridgehead vinyl carbons (C15–C16) and bridge nitrogens (N5–N6) are 6.18 and 5.14 Å, respectively.

One final feature of this structure which should be mentioned is the "*lid-on*" orientation of the *m*-xylene groups at the bridge nitrogen atoms. This is the predicted orientation for the dimers based on steric and NMR considerations as described earlier.

Experimental Section

Physical Measurements. Elemental analyses were performed by Galbraith Labs., Inc., Knoxville, TN. Conductance measurements were obtained in acetonitrile by using an Industrial Instruments, Inc., Model RC 16B conductivity bridge and a cell having cell constant of 0.110 cm^{-1} at 1000 cycles/s. Routine electronic spectra were measured on a Cary 17D recording spectrophotometer using matched 1-cm quartz cells. Infrared spectra were measured in the solid state as Nujol mulls pressed between potassium bromide plates and in solution by using matched demountable cells having Irtran II windows of 0.5-mm pathlength with use of either a Perkin-Elmer Model 457 or 283B infrared spectrophotometer in the region from 4000 to 400 cm^{-1}. Mass spectra were obtained with an MS-9 mass spectrometer at 70 eV.

Proton NMR spectra were obtained with a Varian Associates 360-L spectrometer operating at 60 MHz. ^{13}C NMR spectra were recorded on either Bruker WP-80 or HX-90 spectrometer operating in the Fourier transform mode at 20 or 22 MHz, respectively. ^{13}C NMR spectra were generally obtained by using broad band proton decoupling as well as off-resonance (CW) decoupling. Deuterated solvents were used throughout, and chemical shifts were assigned relative to an internal Me_4Si standard.

The apparatus used for electrochemical measurements was a Princeton Applied Research Corp. potentiostate galvanostat, Model 173, equipped with a Model 175 linear programmer and a Model 179 digital coulometer. Current vs. potential curves were measured on a Houston Instruments Model 2000 X-Y recorder. All measurements were performed in a Vacuum Atmospheres glovebox under an atmosphere of dry, oxygen-free nitrogen. The working electrode for voltametric curves was a platinum disk electrode, with potentials measured vs. a silver wire immersed in an acetonitrile solution of 0.1 M silver nitrate as reference. The working electrode was spun at 600 rpm by a synchronous motor for the rotating platinum electrode (RPE) voltamograms. Peak potentials

(E_p) were measured from cyclic voltamograms measured at 50-mV/s scan rate. Half-wave potentials ($E_{1/2}$) were taken as the potential at half the height of the voltamogram obtained by using the RPE. The value of $|E_{3/4} - E_{1/4}|$ was used as a measure of the reversibility of the couple and was also obtained by using the RPE. For all measurements, the solution contained 0.1 M tetra-*n*-butylammonium tetrafluoroborate as supporting electrolyte.

Molecular weights were determined in benzene or chloroform at 37 °C with a Mechrolab vapor pressure osmometer, Model 301A.

(2,6,7,11,13,19,21,25,26,30,32,38,53,54,55,56-Hexadecamethyl-3,10,14,18,22,29,33,37,40,44,47,51-dodecaazapentacyclo-[29.7.7.7^{12,20}.2^{5,8}.2^{24,27}]hexapentaconta-1,5,7,11,13,18,20,24,26,30,32,-37,39,44,46,51,53,55-octadeceneN$_8$)dinickel(II) Hexafluorophosphate ([Ni$_2${(**duryl(NHEthi)$_2$)Me$_2$[16]tetraeneN$_4$**}$_2$](PF$_6$)$_4$). To a solution of 2.0 g (3.1 mmol) of [Ni{(NH$_2$Ethi)$_2$Me$_2$[16]tetraeneN$_4$}]I$_2$ dissolved in 250 mL of methanol was added a solution prepared by the reaction of 0.16 g (7.0 mmol) of sodium metal with 10 mL of methanol. The solution was heated to reflux, and a solution of 0.80 g (3.5 mmol) of 3,6-bis-(chloromethyl)durene (Pflatz and Bauer) dissolved in 100 mL of dichloromethane and 50 mL of methanol was added dropwise over a period of 4 h. When the addition was complete, the volume of the solution was reduced to 100 mL and 5.0 g (30.7 mmol) of ammonium hexafluorophosphate in methanol was added dropwise to yield the yellow product. Addition of ethanol resulted in the formation of additional product which was collected and dried in vacuo. Yield: 0.9 g (35%). Anal. Calcd for [NiC$_{30}$H$_{44}$N$_6$P$_2$F$_{12}$]: C, 43.03; H, 5.30; N, 10.04. Found: C, 42.70; H, 5.55; N, 10.14.

(2,3,6,7,10,11,13,19,21,22,25,26,29,30,32,38,53,54,55,56-Eicosamethyl-3,10,14,18,22,29,33,37,40,44,47,51-dodecaazapentacyclo-[29.7.7.7^{12,20}.2^{5,8}.2^{24,27}]hexapentaconta-1,5,7,11,13,18,20,24,26,30,32,-37,39,44,46,51,53,55-octadeceneN$_8$)dinickel(II) Hexafluorophosphate ([Ni$_2${(**duryl(MeNEthi)$_2$)Me$_2$[16]tetraeneN$_4$**}$_2$](PF$_6$)$_4$). To a solution of 3.7 g (5.2 mmol) of [Ni{(MeNHEthi)$_2$Me$_2$[16]tetraeneN$_4$}](PF$_6$)$_2$ dissolved in 250 mL of acetonitrile was added a solution prepared by the reaction of 0.24 g (10.4 mmol) of sodium metal with 10 mL of methanol. The solution was heated to reflux, and a solution of 1.20 g (5.2 mmol) of 3,6-bis(chloromethyl)durene dissolved in 250 mL of acetonitrile was added dropwise over a period of 12 h. The solution was cooled, and the white sodium chloride was filtered off. The volume of the solution was reduced to 100 mL, and 4.0 g (24.5 mmol) of ammonium hexafluorophosphate in 100 mL of ethanol was added. Further volume reduction resulted in formation of the yellow product. Recrystallation from an acetonitrile/ethanol mixture yielded the yellow crystals which were collected and dried in vacuo. Yield: 4.2 g (93%). Anal. Calcd for [NiC$_{32}$H$_{48}$N$_6$P$_2$F$_{12}$]$_2$: C, 44.41; N, 5.59; N, 9.71. Found: C, 44.57; H, 5.72; N, 9.53.

(2,7,9,15,17,22,24,30-Octamethyl-3,6,10,14,18,21,25,29,32,36,39,43-dodecaazatricyclo[21.7.7.7^{8,16}]tetratetraconta-1,7,9,14,16,22,24,29,33,38,43-dodecaeneN$_8$)dinickel(II) Hexafluorophosphate ([Ni$_2${(CH$_2$)$_2$-(NHEthi)$_2$Me$_2$[16]**tetraeneN$_4$**}$_2$](PF$_6$)$_4$ **and (2,8,10,16,18,24,26,32-Octamethyl-3,7,11,15,19,23,27,31,34,38,41,45-dodecaazatricyclo-[23.7.7.7^{9,17}]hexatetraconta-1,8,10,15,17,24,26,31,35,38,40,45-dodecaeneN$_8$)dinickel(II) Hexafluorophosphate** ([Ni$_2${(CH$_2$)$_3$(NHEthi)$_2$Me$_2$-[16]**tetraeneN$_4$**}$_2$](PF$_6$)$_4$). These two compounds are produced by the same procedure. The synthesis is presented here for the trimethylene derivative. [Ni{(MeOEthi)$_2$Me$_2$[16]tetraeneN$_4$}](PF$_6$)$_2$ (10 g, 0.014 mol) was dissolved in acetonitrile (500 mL, freshly opened bottle). A solution of the 1,3-diaminopropane (1.04 g, 0.014 mol) in 500 mL of acetonitrile was added dropwise over a 3-h period with continuous stirring. The color changed from yellow-green to a deep brown. The volume of the solution was reduced to about 100 mL (rotovap), and the concentrate was slurried with ~50 mL of powdered silica. The slurry was extracted with acetonitrile, leaving a deep brown residue. The resulting yellow-brown acetonitrile solution was reduced to 25 mL on the rotovap. The solution was applied to a neutral alumina column packed under acetonitrile (2.5 cm × 40 cm). Elution with acetonitrile left a brown band at the top of the column and a yellow band which moved down the column was collected. The volume of the resulting yellow solution was reduced to 25 mL, and ethanol was added to precipitate the complex. *Trimethylene bridge*: yield, 68%. Anal. Calcd for Ni$_2$C$_{42}$H$_{12}$H$_{80}$P$_4$F$_{24}$·0.5CH$_3$CN: C, 35.40; H, 4.80; N, 12.00. Found: C, 35.30; H, 5.13; N, 12.14. *Dimethylene bridge*: yield, 24%. Anal. Calcd for Ni$_2$C$_{40}$N$_{12}$H$_{76}$P$_4$F$_{24}$·CH$_3$CN: C, 34.75; H, 4.75; N, 12.52; Ni, 8.09. Found: C, 34.97; H, 5.05; N, 12.77; Ni, 8.00.

Direct Synthesis of Dimeric (2,10,12,18,20,28,30,36-Octamethyl-3,9,13,17,21,27,31,35,38,42,45,49-dodecaazatricyclo[27.7.7.7^{11,19}]pentaconta-1,10,12,17,19,28,30,35,37,42,44,49-dodecaeneN$_8$)dinickel(II) ([Ni$_2${(CH$_2$)$_5$(NHEthi)$_2$Me$_2$[16]**tetraeneN$_4$**}$_2$](PF$_6$)$_4$). Seven grams of [Ni{(MeOEthi)$_2$Me$_2$[16]tetraeneN$_4$}](PF$_6$)$_2$ dissolved in 500 mL of CH$_3$CN was dropped into 18.3 g of 1,5-diaminopentane (10:1 excess) in 100 mL of CH$_3$CN over a period of 4 h producing an orange-red solution. The volume was rotovaped to ~100 mL and methanol/water was (50/50) added. Rotary evaporation gave a red oil. The oil was dissolved in methanol containing an excess of NH$_4$PF$_6$. Reduction in volume to ~150 mL followed by cooling overnight produced a yellow-brown solid. Repeated dissolving and rotovapping in ethanol/water containing NH$_4$PF$_6$ gave a yellow solid (2.0 g) that was dried in vacuo. This noncrystalline intermediate appeared to contain protonated free amine groups. Anal. Calcd for NiC$_{28}$H$_{52}$N$_8$(PF$_6$)$_2$(HPF$_6$)$_2$: C, 27.95; H, 5.04; N, 9.65. Found: C, 28.13; H, 5.06; N, 9.37.

The dimer was prepared from the protonated bis(diamine) by first liberating the amino groups by the addition of 2 equiv of sodium methoxide under N$_2$ in CH$_3$CN/CH$_3$OH solution. The solution containing the complex of the free bis(diamine) ligand and a solution of [Ni{(CH$_3$OEthi)$_2$Me$_2$[16]tetraeneN$_4$}](PF$_6$)$_2$ were added dropwise simultaneously to a stirred volume of CH$_3$CN. The resulting yellow-brown solution was worked as described above for other synthetic routes. The yellow band collected from the alumina column was diluted with ethanol and evaporated, yielding a yellow solid that was filtered, washed with ethanol and ether, and dried in vacuo. Yield: 50%.

Crystal Structure Analysis of [Ni$_2${(*m*-xylyl(NHEthi)$_2$)Me$_2$[16]tetraeneN$_4$}$_2$](PF$_6$)$_4$·4CH$_3$COCH$_3$. Pale transparent yellow crystals of the PF$_6^-$ salt of the cationic complex, prepared by our previously reported procedure,[11] were grown by slow evaporation from acetone solutions. Two distinct morphologies, truncated square pyramids and very fine, long needles, were present. A small (0.25 × 0.25 × 0.35 mm) crystal of the first variety was mounted on a quartz fiber and coated with several thin layers of epoxy cement for use in the structure determination. Cell constants were determined by least-squares fit of the carefully optimized diffractometer setting angles for 15 reflections having $10.2° \le 2\theta \le 16.5°$ (λ(Mo K$\bar{\alpha}$ = 0.71069 Å). These results and other important crystal data are summarized in Table V. The systematic absences (*hk*0, *h* = odd; *h*0*l*, *l* = odd; 0*kl*, *k* = odd) permitted the unambiguous assignment of the space group as the orthorhombic *Pbca*; the centric nature of the space group was subsequently verified by the intensity and *E* statistics.

The intensity data were collected on a Syntex P$\bar{1}$ automated four-circle diffractometer using the ω–2θ scan technique, graphite-monochromatized Mo K$\bar{\alpha}$ radiation, and scan rates which were assigned depending upon quick premeasurements of peak intensity (intense reflections were measured at 8.0° 2θ/min and weak reflections at 2.0° 2θ/min). Backgrounds were counted at each end of each scan, for a total of half the time spent in the scan. The intensities of ten check reflections were remeasured periodically during the course of the data collection to monitor the crystal condition and orientation and the stability of the instrument. The check reflection intensities showed no significant variation over the 511 h of X-ray exposure required for the data collection. All reflections in the positive *hkl* octant having $4.0° \le 2\theta \le 60.0°$ were measured at least once; the reflections having $30.0° \le 2\theta \le 50.0°$ were all remeasured at a scan

Table V. Crystal Data for Ni$_2$C$_{64}$H$_{96}$N$_{12}$O$_4$P$_4$F$_{24}$

fw = 1794.82 F_{000} = 3712 e
space group: *Pbca* (D_{2h}^{15}, No. 61)
cell constants at 20 (1) °C:
a = 16.353 (5) Å
b = 20.173 (5) Å
c = 24.157 (6) Å
v = 7969 (4) Å^3
ρ_{calcd} (*Z* = 4) = 1.496 (8) g cm^{-3}
ρ_{obsd}[a] (CBr$_3$H/C$_6$H$_6$) = 1.44 (1) g cm^{-3}
λ(Mo K$\bar{\alpha}$) = 0.71069 Å
μ(Mo K$\bar{\alpha}$) = 6.54 cm^{-1}
$e^{-\mu r}$(max)(estd) ≃0.72
$e^{-\mu r}$(min)(estd) ≃0.85
no. independent data = 7104
no. with $I \geq 2\sigma(I)$ = 2503
no. with $I \geq 3\sigma(I)$ = 2123
no. of parameters in LS = 496

	data		
	all	$I \geq 2\sigma(I)$	$I \geq 3\sigma(I)$
R(*F*)	0.218	0.161	0.135
$R_w(F^2)$	0.243	0.223	0.214
GOF	2.09	2.89	3.21
data/parameter ratio	14.3	5.0	4.3

[a] The experimental density was obtained by using a mixture of the two forms of crystals. The disagreement may be a consequence of this or may be due to loss of acetone of crystallization into the flotation medium.

rate of 1.5° 2θ/min in an attempt to improve the signal/noise ratio. Many of the data were very weak. The estimated standard deviations in the reduced intensities (F^2) were calculated by using $\sigma(F^2) = (r/Lp)[S + G^2(B_1 + B_2) + (pI)^2]^{1/2}$, where r is the scan rate, Lp is the Lorentz–polarization correction, S, B_1, and B_2 are the scan and background counts, G is the ratio of scan time to total background counting time (=2.0), I is the net intensity ($=S - G(B_1 + B_2)$), and p is a factor, here chosen as 0.02 on the basis of our prior experience with this instrument, included in a term presumed to represent that component of the total error expected to be proportional to the diffracted intensity.[17] Excluding check reflections, a total of 13057 intensities were measured, of which 7104 were unique and remained after averaging of multiply measured and symmetry equivalent data. Of these, but 2123 possessed intenities greater than 3σ above background. The general weakness of the data is reflected in the much higher than usual values of the internal self-consistency indices for the multiply measured data: $R'(F) = 0.11$ and $R_w'(F^2) = 0.11$.[18] As most of the contributors to these indices were from the higher 2θ angles and consequently were derived from the weakest part of the data, the higher than normal values of $R'(F)$ and $R_w'(F^2)$ were not unexpected The data were reduced in the usual way, being corrected for Lorentz and polarization effects and placed on an absolute scale by means of a Wilson plot. No absorption corrections were made, in view of the low values of μr, the nearly isotropic shape of the crystal and, ultimately, the discovery of the poor quality of the data.

Using only the data having $F^2 > 2\sigma(F^2)$, the structure was solved by the heavy-atom Patterson method. The nickel atom position was used to calculate phases for a Fourier map which yielded positions for a portion of the macrocyclic nitrogen and carbon atoms.[19] The remainder of the structure was gradually elucidated by a series of five structure factor/Fourier and difference Fourier calculations.[20] After several cycles of least-squares refinement, two independent acetone molecules of crystallization were discerned in a difference map and included in the structure with their populations as least-squares variables. Refinement to convergence with all atoms assigned isotropic temperature factors except for the Ni(II) ion led to $R(F)$ of 0.192.[21] As the acetone group populations converged near 1.0, they were subsequently included at full occupancy to help minimize the number of least-squares variables. In the final least-squares refinement cycles, all but four methyl carbon atoms (C13, C14, C17, C18) were assigned anisotropic thermal parameters. Convergence, judged by all parameter shifts being less than one-fourth esd, was achieved with $R(F) = 0.161$, $R_w(F^2) = 0.223$, and GOF = 2.89, for data having $F^2 > 2\sigma(F^2)$. Three cycles of least squares, calculated by using all 7104 unique data, converged at $R(F) = 0.218$, $R_w(F^2) = 0.243$, and GOF = 2.09. A difference Fourier map calculated at this point in an attempt to locate hydrogen atoms revealed a number of peaks of about 1.5 e/Å^3, particularly in the regions of the hexafluorophosphate anions. These large residual peaks and the large and highly anisotropic thermal parameters of the anions, of the acetone solvate molecules, and of some atoms of the cation indicated a complex and extensive static and/or dynamic disorder. Attempts to model the disorder in several ways, including partial occupancy PF_6^- groups in alternative orientations, were entirely unsuccessful. Attempts to develop more complicated models for the disorder were abandoned as they would have led to unacceptably low data/parameter ratios. The refinement was accordingly halted at this point. Due to the poor quality and low amount of significant data, any further investment of effort was deemed unwarranted. A sustained effort to obtain crystals of different anion salts was unsuccessful; only PF_6^- provided crystals and then only in one particular batch of material. The final values of the least-squares refined parameters and the observed and calculated structure amplitudes are included as supplementary material.

As can be seen from the lengths of chemically equivalent bonds (in Table III), the quality of the resulting structure is not particularly accurate, and except for the proof of the molecule's dimeric structure and its overall conformation, few conclusions can be drawn from the details of the results. Because of the unusually high values of the disagreement indices, we were particularly sensitive to the question of the overall reliability of the structure and took great pains in our study to explore (a) alternative solutions to the phase problem[19,24] and (b) the reasons for the high disagreement indices. Lest the reader dismiss our structure on the basis of the above reported R factors for all the data,[26] we have included in Table V the R factors for two sets of the most significant of the data. It is clear that the fit for the most intense data is much better, as it should be if the weaker data are successively excluded (the weak data contribute almost equally to the numerator and to the denominator of the R factor expression). In this case, the "goodness of fit", or GOF, which is analogous to a scaled χ^2, whose optimal value is 1.000, is a better indicator of the overall quality of the fit than are the various R factors. The R factor, quite simply, is a measure of the disagreement between the true structure and the least-squares "model". In this structure we have disordered PF_6^- anions and acetone of crystallization, both of which evidence very high and very anisotropic thermal motion. It is difficult, without introducing a very large number of extra parameters (either as additional, partial occupancy groups or by a higher cumulant thermal motion model[28]), to improve the fit between the true and "model" structure. When one considers that fully 44% of the scattering electron density in the unit cell is comprised by the PF_6^- anions and the acetone groups, our inability to model these groups, under the constraints of a weak data set of limited quality, is understandable and the resultant higher than desirable R factors are explicated. Insofar as we have herein interpreted it, we are confident that the structure we report here has been correctly solved and is in fact the true structure.

Acknowledgment. The support of these studies by grants from the National Science Foundation is gratefully acknowledged. The assistance of Dr. Charles Cottrell in obtaining some of the NMR results is greatly appreciated. G.G.C. gratefully acknowledges support from the Dreyfus Foundation as a Teacher-Scholar Awardee.

Supplementary Material Available: Listing of least squares parameters and observed and calculated structure amplitudes (18 pages). Ordering information is given on any current masthead page.

(17) Busing, W. E.; Levy, H. A. *J. Chem. Phys.* **1957**, *26*, 563–568.

(18) The definitions of the various disagreement indices are: $R'(F) = \{\sum_{hkl}\sum_j^n||F_{hkl_{av}}| - |F_{hkl_j}||\}/\{\sum_{hkl}n\cdot|F_{hkl_{av}}|\}$ and $R_w'(F^2) = [\{\sum_{hkl}\sum_j^n[(F_{hkl_{av}}{}^2 - F_{hkl_j}{}^2)^2/\sigma^2(F_{hkl_{av}}{}^2 - F_{hkl_j}{}^2)]\}/\{\sum_{hkl}\sum_j^n[F_{hkl_{av}}{}^4/\sigma^2(F_{hkl_{av}}{}^2 - F_{hkl_j}{}^2)]\}]^{1/2}$ where n is the number of j measurements F_{hkl_j} contributing to the averages: $F_{hkl_{av}} = \{\sum_j^n F_{hkl_j}\}/n$ and $F_{hkl_{av}}{}^2 = \{\sum_j^n[F_{hkl_j}{}^2/\sigma^2(F_{hkl_j}{}^2)]\}/\{\sum_j^n\sigma^{-2}(F_{hkl_j}{}^2)\}$ where F_{hkl_j} and $F_{hkl_j}{}^2$ are the observed values for measurements j.

(19) The elucidation of the structure was not straightforward. No reasonable ligand or anion fragments and only three of the four nitrogen atoms coordinated to the Ni(II) center were present on the first Fourier map and at rather different Ni–N distances. For a centric structure, such behavior is totally foreign to our experience, and this map was set aside while we systematically searched for possible solutions using all orthorhombic space groups belonging to the same class of successively lower symmetry and with all permutations of the cell axes. None of these produced reasonable structure fragments, and, for many, the Patterson solutions themselves were inconsistent with the number of asymmetric units present in the cell. Because of these negative results, after several months of concentrated effort, the whole determination was shelved for approximately 1 year while efforts were focused on finding chemical and spectroscopic means to solve the isomer problem. It is wholly to the credit of L.L.Z. that the structure was finally solved, proceeding in very dogged fashion from the first Fourier we had generated in space group *Pbca*. It is clear from the poor quality of the results why so much difficulty was experienced in the solution. In retrospect, the data set was too weak (although we have easily solved other, equal-atom, structures with similarly weak data sets), presumably as a direct consequence of the large disorder, large apparent thermal motion, and (probably) poor long-range order in the crystal.

(20) The programs used in this study were primarily from the CRYM crystallographic computing system.[21] The atomic form factors were from a standard source.[23]

(21) DuChamp, D. J., Paper B14, Program and Abstracts, American Crystallographic Association Meeting, Bozeman, MT, 1964.

(22) The usual R factor indices, where F^o and F_c have the standard meanings and where $w = \sigma^2(F_o^2)$, are defined as $R(F) = \sum_{hkl}||kF_o| - |F_c||/\sum_{hkl}|kF_o|$, $R_w(F^2) = \{\sum_{hkl}w(k^2F_o^2 - F_c^2)^2/\sum_{hkl}wk^2F_o^4\}^{1/2}$, and GOF = $\{\sum_{hkl}w(k^2F_o^2 - F_c^2)^2/(n_o - n_p)^2\}^{1/2}$. The function minimized in the least-squares refinement was $\sum_{hkl}w(k^2F_o^2 - F_c^2)^2$.

(23) "International Tables for X-Ray Crystallography"; Kynoch Press: Birmingham, England, 1962; Vol. III, pp 202–203.

(24) The crystallographic errors cited by Shomaker and Marsh[25] in their reanalysis of seven crystal structures in the Vol 16 (1977) issues of *Inorganic Chemistry* are misassignments of the space group. In footnote 19, above, we recount some of our efforts to explore alternative space group choices. Normally the absences consistent with *Pbca* and the presence of a center of symmetry demonstrated by the E statistics would be unrefutable. We have seen cases, however, where either the absences or the E statistics have been misleading and so did undertake the exploration of lower symmetry space groups. That we succeeded in solving the structure only in *Pbca* gives us confidence that we have *the* correct structure solution.

(25) Marsh, R. E.; Shomaker, V. *Inorg. Chem.* **1979**, *18*, 2331–2336.

(26) There are sound theoretical reasons for using *all* of the data rather than only the data $>3\sigma$ above background, in the refinements; this practice avoids systematic bias in the data and presumably in the results.[27]

(27) Hirshfeld, F. L.; Rabinovich, D. *Acta Crystallogr., Sect. A* **1973**, *A29*, 510–513. Arnberg, L.; Hovmoeller, S.; Westman, S. *Ibid.* **1979**, *A35*, 497–499. French, S.; Wilson, K. *Ibid.* **1978**, *A34*, 517–525.

(28) Johnson, C. K. In "Thermal Neutron Diffraction"; Willis, B. T. M., Ed.; Oxford University Press: Oxford, 1970; pp 132–160.